ELSEVIER

Journal of Chromatography A, 949 (2002) 307–326

JOURNAL OF CHROMATOGRAPHY A

www.elsevier.com/locate/chroma

Analysis of linear and cyclic oligomers in polyamide-6 without sample preparation by liquid chromatography using the sandwich injection method
III. Separation mechanism and gradient optimization

Y. Mengerink[a,*], R. Peters[a], Sj. van der Wal[a], H.A. Claessens[b], C.A. Cramers[b]

[a]*Ml&Q, DSM Research, P.O. Box 18, 6160 MD Geleen, Netherlands*

[b]*Laboratory of Instrumental Analysis, Eindhoven University of Technology, P.O. Box 513, 5600 MB Eindhoven, Netherlands*

Abstract

The first six linear and cyclic oligomers of polyamide-6 can be quantitatively determined in the polymer using HPLC with the sandwich injection method and an aqueous acetonitrile gradient. In this final part of the triptych concerning the determination of the oligomers in polyamide-6, the irregular elution behavior of the cyclic monomer compared to the cyclic oligomers was investigated. We also optimized the separation of the involved polyamide oligomers, with respect to gradient steepness, stationary phase, column temperature and mobile phase pH. The irregular elution behavior of the cyclic monomer could be caused by its relatively large exposed/accessible hydrophobic surface, which permits relatively easy penetration into the hydrophobic stationary phase giving extra retention. The dipole moment of the different oligomers was used as a measure for this exposed/accessible hydrophobic area to correlate the retention factors using quantitative structure–retention relationships. We also studied the retention behavior of the polyamide, which is injected each run directly onto the column and modifies the stationary phase. Using a 250-μl post gradient injection zone of formic acid on a 250×3 mm Zorbax SB-C_{18} column, the polyamide could be effectively removed from the stationary phase after each separation. The linear solvent strength (LSS) model was used to optimize the separation of the first six linear and cyclic oligomers. As the LSS model assumes a linear correlation between the modifier concentration and the logarithm of the retention factor and the cyclic monomer and dimer show extreme curvation of this relation in the eluting region, we investigated different models to predict gradient elution from isocratic data. A direct translation of the isocratic data to gradient retention times did not yield adequate retention times using the LSS model. It was found that the LSS model worked acceptably if gradient retention times were used as input data. Even for fast non-linearly eluting components, an average error of 0.4 resolution units of 4σ was obtained. Using the LSS model in combination with different column temperatures and mobile phase pH values, a separation of the first six linear and cyclic oligomers was accomplished. © 2002 Elsevier Science B.V. All rights reserved.

Keywords: Sandwich injection; Injection methods; Gradient elution; Optimization; Oligomers; Polymers; Polyamide

1. Introduction

Polyamide-6 (nylon-6) is a synthetic polymer with a hexane amide backbone. Beside the linear polymer with a carboxylic acid and a primary amine end-

*Corresponding author. Tel.: +31-46-476-1632; fax: +31-46-476-1127.

E-mail address: ynze.mengerink@dsm-group.com (Y. Mengerink).

0021-9673/02/$ – see front matter © 2002 Elsevier Science B.V. All rights reserved.
PII: S0021-9673(01)01440-6

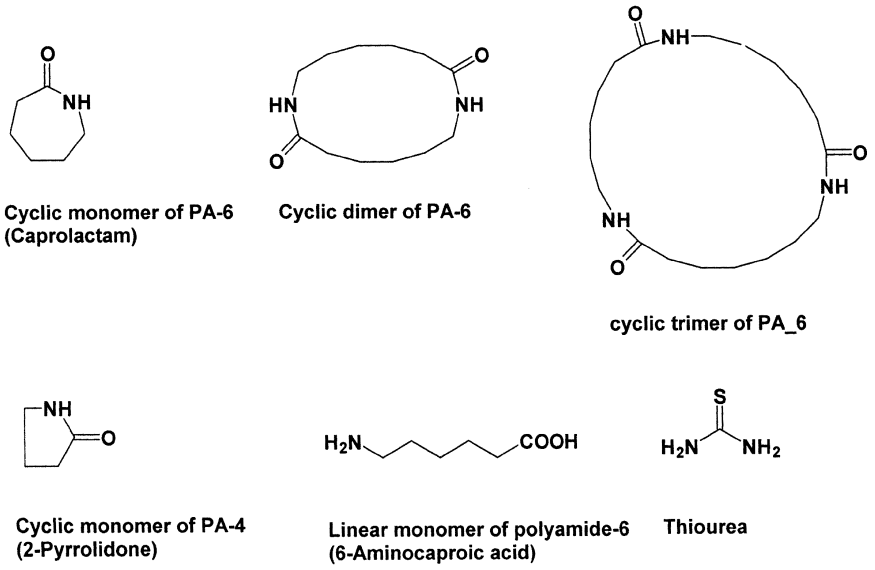

Fig. 1. Structures.

group, cyclic structures exist (Fig. 1). To determine the linear and cyclic oligomers (including up to $n=6$) in nylon-6, the sandwich injection method and group equivalent detection were described in parts I and II, respectively [1,2].

Elution behavior of oligomeric series often obeys simple elution characteristics, where the monomer elutes first and the higher oligomers succeed each other. The linear oligomers of polyamide-6 follow this elution pattern [Fig. 2a fluorescence signal (L1–L6)]. For isocratic chromatographic conditions, this can be described by the Martin equation [3]:

$$\ln k = a_0 + a_1 n \quad (1)$$

where k is the retention factor ($k = (t_r - t_0)/t_0$, where t_r is the retention time of the oligomers and t_0 is the retention time of an unretained component), a_0 and a_1 are constants and n is the number of backbone units of the oligomeric series.

When the end-group of an oligomeric series promotes retention and the backbone promotes elution, a reversed elution pattern will be obtained, where the monomer elutes last ($a_1 < 0$). Again, the elution order of the higher oligomers succeeds each other [4,5]. However, as has been observed in parts I and II and by other authors also, the cyclic oligomers of polyamide-6 show a deviant elution behavior on a reversed-phase stationary phase (see Fig. 2 UV signal and Fig. 3a) [1,2,6–9]. The cyclic dimer (C2) elutes first, the cyclic monomer (C1) thereafter and the cyclic trimer (C3) elutes third. From hereon the successive higher oligomers succeed each other. No satisfactory explanation has been given in the literature for this irregular elution behavior of the cyclic oligomers of polyamide-6.

Different models are available to predict retention in reversed-phase HPLC based on molecular characteristics. Galushko describes a simple and straightforward model based on Horvath's solvation model [10–14] which is given in Eq. (2):

$$\ln k = aV^{2/3} + b\Delta G_{es} + c \quad (2)$$

a, b and c represent three constants for a given mobile phase–stationary phase combination [11,12], ΔG_{es} is the difference of the electrostatic Gibbs free energy of the solute in the mobile and stationary phase and V is the molar volume of the solute. The molecular volume of the molecule can be estimated using the partial molar volumes of the fragments. The same holds for the electrostatic Gibbs free energy. Some of these values, which are of interest for the cyclic molecules investigated are given in Table 1 [10].

The Galushko equation is already a start to a more

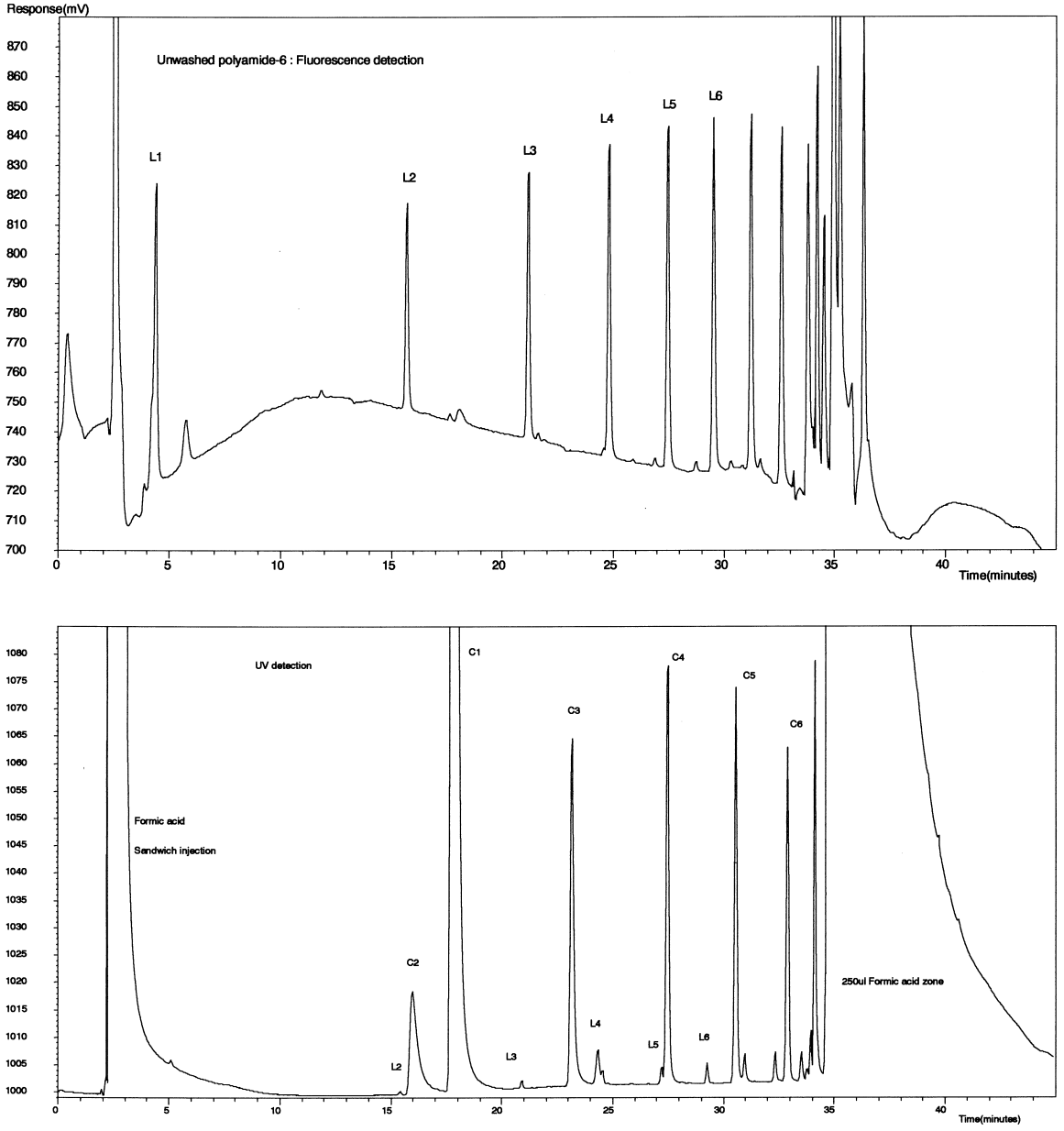

Fig. 2. Optimized HPLC conditions and chromatogram: 20 mg unwashed polyamide/ml formic acid injected using sandwich injection (2 μl formic acid zone–3 μl sample–2 μl formic acid zone). Column 250×3 mm Zorbax SB-C_{18} (5 μm, 80 Å, temperature=40°C). Mobile phases, A: 10 m*M* H_3PO_4, pH 2.6 (NaOH); B: acetonitrile; gradient $t_{0\ min}$ 99% A–1% B, $t_{36\ min}$ 68% A–32% B. Flow, 0.51 ml/min. UV detection λ=200 and 220 nm. At $t_{31\ min}$ post gradient injection of 250 μl formic acid. Post-column reaction detection: Reagent 38 g sodium tetraborate, 3 g sodium hydroxide and 1 ml 3-mercaptopropionic acid dissolved in 1 l water to which 0.8 g orthophthalaldehyde in 20 ml methanol is added. Post-column flow-rate, 0.25 ml/min, Polyether ether ketone (PEEK) capillary 0.25 mm×3 m. Fluorescence detection λ_{ex}=330 nm, λ_{em}=420 nm. At $t_{31\ min}$ injection of 250 μl formic acid to clean the stationary phase. (a) Fluorescence signal of the derivatized linear oligomers (L1=linear monomer, L2=linear dimer, etc.). (b) UV signal of the linear and cyclic oligomers (C1=cyclic monomer, C2=cyclic dimer, etc.).

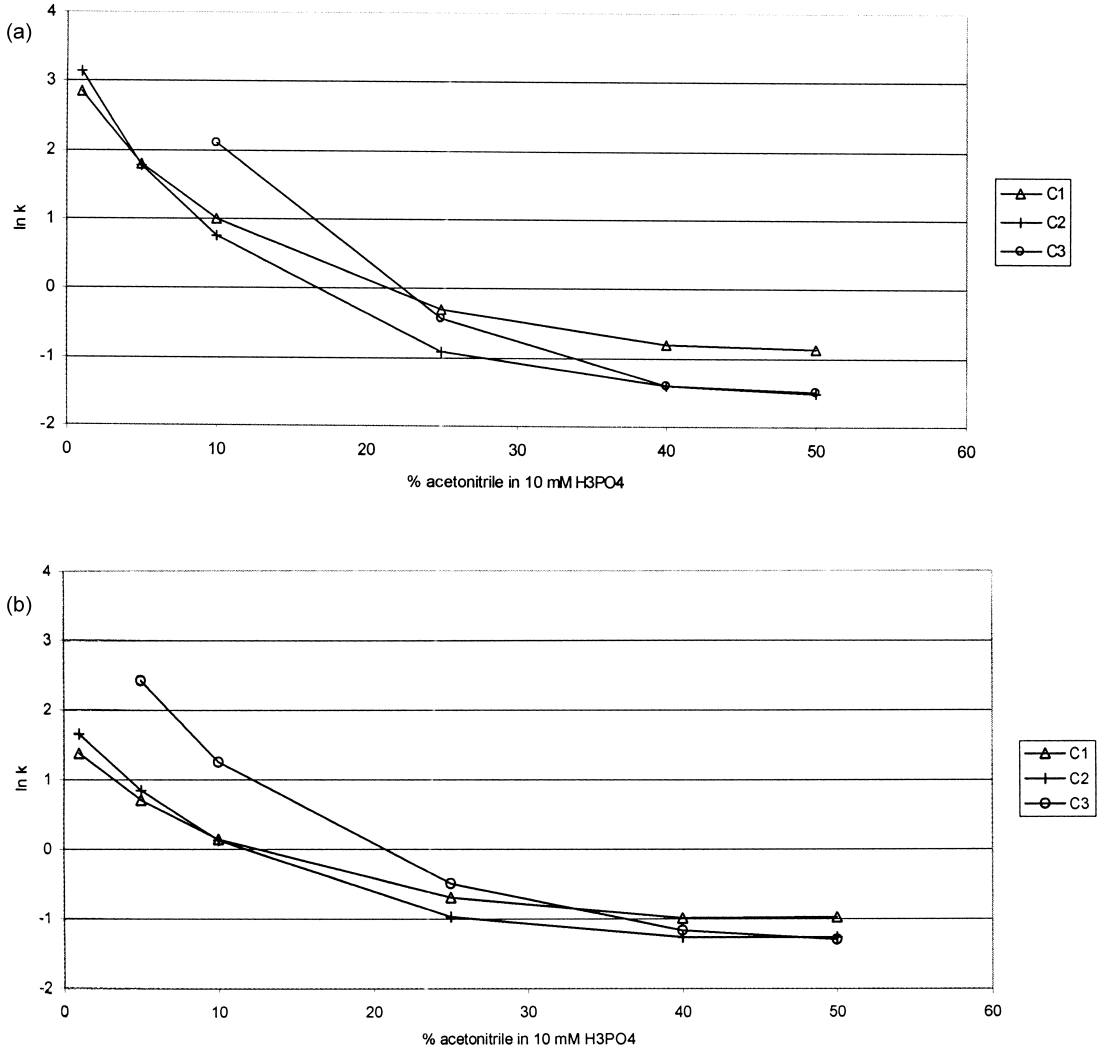

Fig. 3. (a) Elution characteristics of the cyclic monomer (C1), cyclic dimer (C2) and cyclic trimer (C3) of polyamide-6 oligomers on Nucleosil-120-5C_{18} at RT. (b) Elution characteristics of the cyclic oligomers of polyamide-6 on Nucleosil-120-5C_4 at RT.

Table 1
Contribution of different molecule fragments on the molecular volume and electrostatic free Gibbs energy, based on Refs. [10–12]

Fragment	V_i (m^3/mol)	$\Delta G_{e.s.\ H2O}$ (J/mol)
CH_2	0.000016	2.84
C=O	0.000013	32.20
NH	0.000007	19.20

chemometric approach, which is also known as quantitative structure–retention relation (QSRR), as recently reviewed by Kaliszan [15]. This approach in principle applies all kind of relevant molecular descriptors to model retention. QSRR was used in combination with different experimental conditions to investigate the irregular elution behavior of the first eluting cyclic oligomers.

Using the sandwich injection method the complete polyamide-6 sample is injected on the stationary

phase [1]. As most of the polyamide remains on the stationary phase, it gets more or less modified, resulting in poor peak shapes of the separated oligomers. Therefore, we also investigated the retention mechanism of this injected polyamide on the stationary phase using an aqueous acetonitrile mobile phase and multiple injections of formic acid zones to try to circumvent this stationary phase modification problem.

In a typical polyamide-6 sample, the amount of linear oligomers is an order of magnitude smaller compared to the amount of cyclic oligomers. For such samples it is not important if a linear oligomer coelutes with a cyclic oligomer as the linear oligomers are selectively detected by post-column derivatization. However, an optimization of the separation would open the possibility to analyze all oligomeric mixtures, even with equal amounts of linear and cyclic oligomers. To perform such an optimization the use of a computer program is mandatory [16]. Commercially available gradient optimization programs use solely the so-called linear solvent strength (LSS) theory to optimize gradient separations from gradient input data [17–20]. To predict gradient separation from isocratic data, quadratic or higher models are also available. The LSS model assumes a linear relation between the logarithm of the retention factor k and the organic modifier concentration ($\varphi_{\mathrm{modifier}}$). To optimize complex mixtures a combination of gradient optimization and a second optimization parameter like, for example, the column temperature can be used [21–29]. As the separation of six linear and six cyclic oligomers is very complex we investigated the accuracy and precision of this LSS model. The first problem which has been described is the nonlinear retention behavior ($\ln k$ vs. $\varphi_{\mathrm{modifier}}$) [23,30,31]. In particular, the retention factors of the cyclic monomer and dimer, which elute in the low organic modifier concentration region, show a significant non-linearity. Comparing the non-linearity study of Schoenmakers, where a quadratic solvent strength (QSS) model was investigated ($\ln k = \mathrm{A0} + \mathrm{A1}\varphi + \mathrm{A2}\varphi^2$), the investigated A2 value lies between 0 and 20, where for the cyclic monomer and dimer at a C_{18} bonded phase with acetonitrile as a modifier, A2 values of 50–70 were obtained [31] (Fig. 3a). No data were found in literature to prove a good fit of the LSS model for gradient optimization of such kind of fast non-linearly eluting components. Other in-column factors could also influence the accuracy of the LSS model [30]. Some important in-column factors (dead-time and equilibration and modifier uptake) were investigated. The dead time determination of the column is not straightforward. The t_0-value of a selected marker is assumed to be constant during the gradient run. However, especially with octadecyl modified silica the measured elution time of a t_0 marker is strongly influenced by mobile phase composition [32]. Beside this dead-volume problem the LSS model assumes an instantaneous equilibration of the organic modifier on the stationary phase. After the dwell time of the system the percentage modifier is assumed to increase immediately. However, due to preferential uptake of the modifier onto the octadecyl modified silica, a kind of extra dwell time is introduced. Kazakevich et al. investigated both effects exhaustively which are related due to the excess adsorption of the modifier on the reversed-phase stationary phase. A maximum excess adsorption of 10 $\mu\mathrm{mol/m^2}$ of acetonitrile on a reversed-phase stationary phase was measured at an initial concentration of 30% acetonitrile in an aqueous mobile phase [33].

To investigate these possible sources of error, we calculated the gradient elution retention time of the cyclic monomer and cyclic dimer directly from the isocratic data, investigated the role of the curvation of the ln k-modifier concentration plot, determined the influence of the dead time and its change with organic modifier concentration and studied the role of modifier equilibration. These calculated gradient retention times from isocratic data were compared with the gradient retention times from experimental gradient data.

In this paper, we attempted to elucidate the irregular elution behavior of the cyclic monomer compared to the higher cyclic oligomers. We also studied the retention behavior of the polyamide, which modifies the stationary phase. To investigate accuracy of the LSS model, we studied the nonlinear behavior of the cyclic monomer and cyclic dimer, the influence of the stationary phase stabilization and the influence of the dead-volume of the system. The LSS model, but also different stationary phases and the influence of pH was used to optimize

the separation of the first six linear and cyclic oligomers.

2. Experimental

All experiments were carried out without the sandwich injection method and without post-column reaction of the primary amines (unless otherwise specified) using an HP1090 liquid chromatograph (Agilent, Waldbronn, Germany). However, the chromatograms (Fig. 2) and the data of Fig. 12 were obtained using a quaternary system, a 900-μl autosampler, a column thermostate module, a diode array detector, an isocratic pump and a fluorescence detector (all Agilent 1100, Waldbronn, Germany). All oligomeric test samples used were laboratory-made. Specific conditions of the optimized chromatographic conditions are given in the caption to Fig. 2. An overview of the investigated stationary phases is given in Table 2. The other experimental conditions are described in Parts I and II [1,2].

Multiple regression equations were solved using the Winstat-add ins (R. Fitch software) of EXCEL97 (Microsoft, Seattle, WA, USA). Gradient optimization programs used were Chromsword version 1.1 (Merck, Darmstadt, Germany) and DryLab version 2.05 (LC Resources, Orinda, CA, USA). All other calculations were performed using EXCEL97 spreadsheets (Microsoft).

The cyclic oligomers of polyamide-6 are abbreviated as Cx and the linear oligomers of polyamide-6 are abbreviated as Lx, where x represents the number of backbone units — [CO-C_5H_{10}-NH]. The cyclic oligomers of other polyamides are abbreviated as Cx-PAy, where y represents the number of carbon atoms which are present in one backbone unit. The cyclic monomer of polyamide-4, which is given in Fig. 1 should be abbreviated as C1-PA4.

3. Results

3.1. Retention mechanism and modeling of the cyclic monomer and cyclic dimer

The elution order of the cyclic monomer compared with its higher cyclic oligomer is irregular (Fig. 2b). Under the given conditions the cyclic monomer is more retained compared to the cyclic dimer, but less compared to the cyclic trimer (Figs. 2b and 3a). No fundamental explanation has been given for this deviating retention elution behavior. So far only Nikolov et al. postulated that only the cyclic monomer was able to penetrate between the C_{18} chains gaining extra retention at higher percentages of modifier [7]. At first sight this is an easy elucidation of the observed retention. However, when the cyclic monomers of different polyamides are injected on a reversed-phase system, they elute under aqueous acetonitrile conditions in a very normal order (Fig. 4,

Table 2
Please supply caption for this table

	dp (μm)	Pore size (Å)	Pore vol (ml/g)	Surf area (m^2/g)	% C	Surface coverage (μmol/m^2)	ρ (g/ml)	Bonded group	End capping
Nucleosil 120-5C_4	5	120	0.65	200				C_4H_9	
Nucleosil 120-5C_{18}	5	120	0.65	200	11	3.6	0.55	$C_{18}H_{37}$	$Si(CH_3)_2$
Nucleosil 50-5	5	50	0.80	420	0	0		–	–
Zorbax RX C_{18}	5.2	80	0.45	180	12	3.3	1	$C_{18}H_{37}$ $(CH_3)_2$	No
Zorbax SB C_{18}	5.2	80	0.45	180	10			$C_{18}H_{37}$ $(C_3H_7)_2$	No
Zorbax Eclipse	5.2		0.45		9.5	3.4		$C_{18}H_{37}$ $(CH_3)_2$	$Si(CH_3)_2$
Zorbax SB C_3	5.2	80	0.45	180	4			$(C_3H_7)_3$	No
Zorbax Bonus	5.2	80	0.45	180	9.5			C_3H_6-NHCO-$C_{13}H_{27}$ $(C_3H_7)_2$	$Si(CH_3)_2$

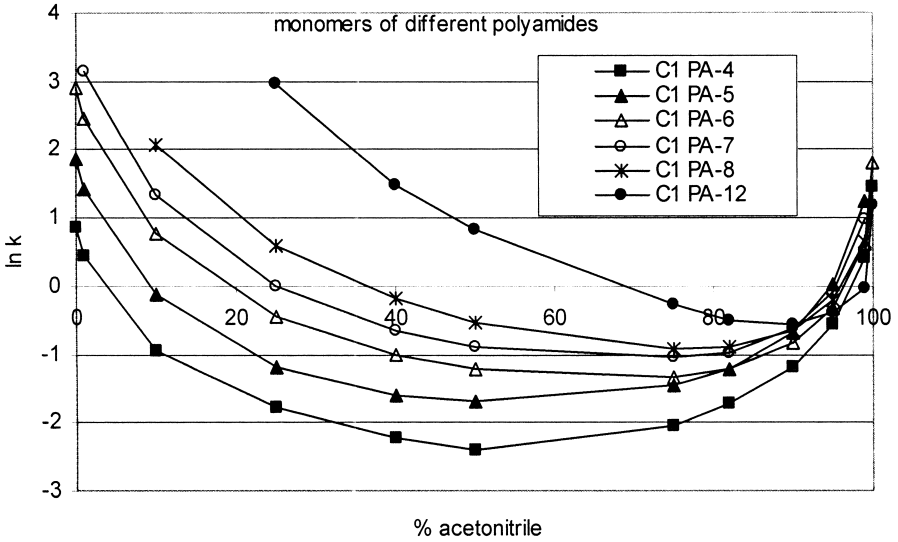

Fig. 4. Elution characteristics of the cyclic monomers of different polyamides on Nucleosil-120-5C_{18}.

viz. C1 of PA-4 elutes first, C1 of PA-5 elutes second, etc.). These results are in contradiction with Nikolov's elucidation. To investigate the interactions of the cyclic monomer and the cyclic dimer with the packing material, different stationary phases were compared (Table 2). All alkyl chain modified phases show coelution at higher acetonitrile concentrations of the cyclic dimer with the cyclic trimer, but a substantial retention of the cyclic monomer comparable to the results in Fig. 3a. However, on less hydrophobic stationary phases (Nucleosil 120-5C_{18}, Nucleosil 120-5C_4 Zorbax Bonus-RP and the Zorbax SB-C_3) [34], the elution order of the cyclic monomer and cyclic dimer reverses at lower percentages of modifier. With the Zorbax RX-C_{18}, Zorbax Eclipse XDB and Zorbax SB-C_{18}, the cyclic dimer still elutes before the cyclic monomer even at 1% acetonitrile. All higher cyclic oligomers ($n=3$–6) elute at higher percentages of modifier before the cyclic monomer and these higher cyclic oligomers are more retained than the cyclic monomer at lower percentages of modifier. The Nucleosil 120-5C_4 and the Nucleosil 120-5C_{18} column show normal elution order at low modifier concentration (cyclic monomer elutes before the cyclic dimer, see Fig. 3a,b). On the C_{18}-phase, reversal of this elution order appears at much lower modifier concentrations than on the C_4 column. With the C_{18}-column, coelution of the cyclic monomer and cyclic dimer occurs at approximately 6% acetonitrile or 10% methanol. With the C_4 column, this coelution occurs at 10% acetonitrile or 20% methanol. By using a non-modified bare silica column (Nucleosil 50-5) an opposite retention behavior was observed (Fig. 5). At higher percentages of acetonitrile, a normal retention behavior is observed, where the cyclic monomer elutes before the cyclic dimer. However, when the mobile phase is completely aqueous a reversal of this elution order is observed. A similar elution behavior was observed with the Zorbax SB-C_3 column and 1,1,1,3,3,3-hexafluoroisopropanol instead of acetonitrile as a modifier, indicating an elution mechanism similar to that of the Nucleosil 50-5 column.

Looking in more detail at the structure of the cyclic monomer and cyclic dimer (Fig. 1), a huge difference in dipole moment can be observed. ($\mu_{\text{cyclic monomer of pa-6}}=3.88$ Debye and $\mu_{\text{cyclic dimer of pa-6}}=2.6$ Debye) [35]. We assume that in reversed-phase systems (non-polar modified silica as a stationary phase and acetonitrile–water as the mobile phase) the relatively large exposed/accessible hydrophobic surface of the monomer permits easy penetration into the hydrophobic stationary phase to occupy a cavity. The cyclic dimer has a smaller exposed/accessible hydrophobic area and its penetration into the stationary phase will be energetically

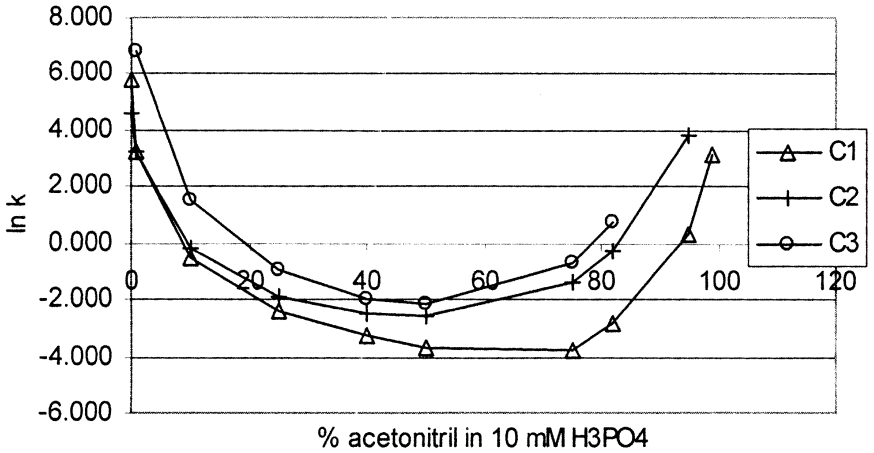

Fig. 5. Elution characteristics of the cyclic oligomers of polyamide-6 on unmodified silica-based stationary phase (Nucleosil 50-5).

less favorable. This also explains the fact that a smaller cyclic monomer (e.g. of polyamide-4 or -5) with a smaller accessible hydrophobic area will penetrate less easily into the non-polar stationary phase. Referring to Horvath's solvation model, it suggests that there is also energy involved in the movement of the molecule from a cavity in the mobile phase to another cavity in the stationary phase. An opposite interaction model could be set-up for a normal-phase system and obviously the propyl modified silica column with HFIP as an organic modifier acts like a normal-phase system.

Attempting to model the retention of the first six cyclic oligomers of polyamide-6 (C1-PA6 to C6-PA6) and six monomers of different polyamides (C1-PA4 till C1-PA8 and C1-PA12), Chromsword was used to estimate the molecular volume and the electrostatic Gibbs free energy (Tables 1 and 3), but a good correlation of Galushko's model given in Eq. (2) was not found (Fig. 6, abc values, see Table 4).

Table 3
Molecular parameters of polyamide monomers and polyamide-6 oligomers

Compound	V (M^3/mol)	ΔG (J/mol)	H-bound acceptor/donor, amide functions	Dipole moment (Debye)	Ln k, experimental on Zorbax SB-C_{18}, % acetonitrile		
					10	25	40
C1–PA-6	1.03×10^{-4}	−68 000	1	3.88	1.04	−0.39	−1.07
C2–PA-6	1.96×10^{-4}	−136 100	2	2.6	0.47	−1.45	−2.06
C3–PA-6	2.89×10^{-4}	−204 100	3	2.5[a]	1.83	−0.83	−2.06
C4–PA-6	3.83×10^{-4}	−272 100	4	2.5[a]	3.04	−0.47	−2.06
C5–PA-6	4.76×10^{-4}	−340 200	5	2.5[a]		−0.12	−2.06
C6–PA-6	5.69×10^{-4}	−408 200	6	2.5[a]		0.22	−2.06
C1–PA-4	7.27×10^{-5}	−62 350	1	3.55	−0.84	−1.76	−2.29
C1–PA-5	8.78×10^{-5}	−65 190	1	3.83	0.06	−1.16	−1.67
C1–PA-6	1.03×10^{-4}	−68 000	1	3.88	1.04	−0.39	−1.07
C1–PA-7	1.18×10^{-4}	−70 870	1	3.86	1.62	−0.01	−0.80
C1–PA-8	1.33×10^{-4}	−73 700	1	3.85	2.41	0.61	−0.72
C1–PA-12	1.94×10^{-4}	−85 070	1	3.65	3.38	3.18	1.56

[a] Indicates the estimated dipole moment of the cyclic trimer, tetramer, pentamer and hexamer of polyamide-6, as these values were not available, as a measure for the exposed/accessible hydrophobic surface, see also text.

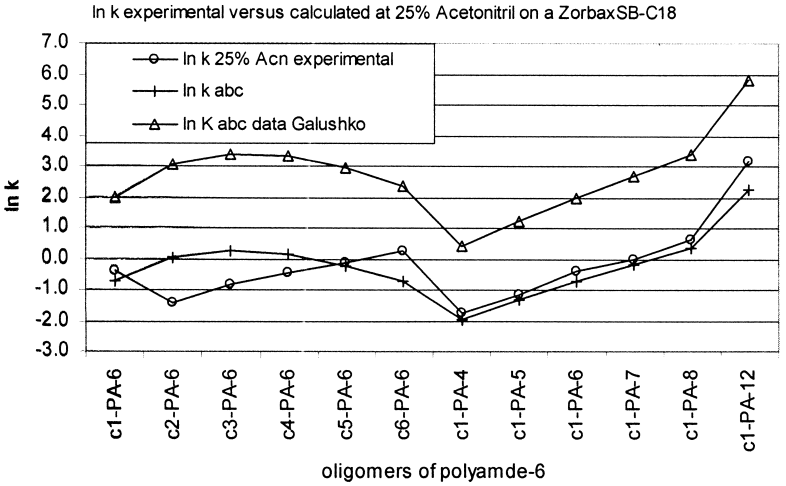

Fig. 6. Experimental data at 25% acetonitrile on a Zorbax SB-C_{18} column. + abc values calculated using the experimentally obtained ln k values. Δ abc data obtained using the test-set of Galushko.

Using the column parameters abc, which were obtained using Galushko's test set [11,12], a rough approximation of the elution window can be obtained, however a deviation of approximately 2 (ln k) units was measured. Even when the abc values were calculated from the retention factors of the cyclic oligomers using multiple regression and although a reasonable correlation was obtained for the cyclic monomers of the different polyamides, the cyclic oligomers of polyamide-6 did not fit (Fig. 6). In QSRR in general, additional parameters could give a better fit. The amount of amide functions was chosen

Table 4
Calculated results of different QSSR models at different acetonitrile concentrations using multiple regression, including the confidence limits at 95%

	Acetonitrile (%)	n	r	a	b	c	d	h
Abc using	10			6140	6.46×10^{-5}	−5.67		
test set	25			4124	5.55×10^{-5}	−3.31		
Galushko	40			2797	4.59×10^{-5}	−2.07		
Abc using	10	9	0.898	3089±1728	$3.80\pm2.71\times10^{-5}$	−3.55±2.52		
the cyclic	25	11	0.817	3267±1883	$4.48\pm2.64\times10^{-5}$	−4.88±2.87		
oligomers	40	11	0.868	2577±1409	$3.96\pm1.97\times10^{-5}$	−4.35±2.15		
Abcd using	10	9	0.992	3545±817	$1.96\pm1.09\times10^{-5}$	−12.1±3.1	2.09±0.72	
the cyclic	25	11	0.974	2789±553	$3.96\pm1.15\times10^{-5}$	−13.1±3.4	2.02±0.77	
oligomers	40	11	0.984	2386±527	$3.57\pm0.78\times10^{-5}$	−10.7±2.3	1.54±0.52	
Abch using	10	9	0.937	−2712±8837	$-38.5\pm9.87\times10^{-5}$	3.09±10.21		−22.0±33.0
the cyclic	25	11	0.990	−2381±1392	$-28.4\pm6.49\times10^{-5}$	2.21±1.80		−23.8±5.45
oligomers	40	11	0.994	−1681±916	$-33.3\pm14.4\times10^{-5}$	0.99±1.18		−17.9±3.58

n = number of oligomers measured in the elution window, r is the correlation coefficient; c is constant, a is the parameter concerning the molecular volume, b is the parameter concerning the electrostatic Gibbs free energy, d is the parameter concerning the dipole moment and h is the parameter concerning the H-bond donor/acceptor function.

to study this influence. The Galushko model was modified resulting in Eq. (3):

$$\ln k = aV^{2/3} + b\Delta G_{es} + c + hH \quad (3)$$

where H is the amount of amide functions and h is the corresponding QSRR parameter (Table 3). Although a better fit was obtained compared to the original model of Galushko, still no good match for the elution characteristics could be found for the different percentages of acetonitrile. In particular, the elution order of the cyclic monomer and cyclic dimer did not fit acceptably (compare in Fig. 7 the calculated abch ln k value of C1-PA6 and C2-PA6 with the experimental ln k values). A substantially better fit was obtained when the dipole moment is used as an additional QSRR parameter for the accessible hydrophobic area of the molecule. As the dipole moment of the cyclic trimer, tetramer, pentamer and hexamer of polyamide-6 are not available in literature, a rough estimation of 2.5 Debye was used (see also Table 3). Although not measured or calculated these seem obvious values as a measure of the hydrophobic exposed/accessible surface, which is thought to be responsible for the deviating elution characteristic of the cyclic monomer. Galushko's equation is now modified to:

$$\ln k = aV^{2/3} + b\Delta G_{es} + c + dD \quad (4)$$

where D is the dipole moment and d is the corresponding QSRR parameter. Using this set of molecular descriptors, very good fits where obtained between the experimental and calculated data. In particular, the elution prediction of the cyclic monomer and dimer is exceptionally good. In Fig. 7 the calculated (abcd) and experimentally obtained ln k value of C1-PA6 and C2-PA6 clearly show this improved agreement.

4. Removal of the retained polyamide polymer

In Part I, we studied the peak broadening of the linear and cyclic oligomers, which occurred after several polymer injections on a new column using the sandwich injection method [1]. By using an acetonitrile gradient, only the first six oligomers eluted with full recovery. Higher oligomers stayed partially on the column and are removed by injecting a formic acid zone at the end of the gradient. However, high-molecular-mass polyamide remains on the column. Due to the formic acid zones injected during the gradient runs, the polyamide does not stay at the top of the column, but slowly moves through the column. Two columns were opened after 60 polymer injections and the packing material of the 25-cm column was divided into 10 portions, each representing 2.5 cm of the column packing material. During refluxing these column fractions were hydrolyzed with heated 6 *M* hydrochloric acid.

6-Aminocaproic acid, the hydrolytic product of polyamide-6 was found distributed along the whole column. It was demonstrated that large amounts of formic acid could be used on a Zorbax SB-C_{18} column without reducing the column performance [36]. The 250×3 mm I.D. Zorbax-SB column was effectively cleaned with a 100-μl formic acid post-gradient injection plug. However, precipitation of the polymer in the post-column reactor occurred after approximately 60 injections. Using a 250-μl formic acid post gradient injection plug this precipitation problem did not occur any more. This indicates that by effectively cleaning the column and the post-column reactor after each run using a Zorbax SB-C_{18} column no efficiency loss was observed. Fig. 2 depicts the chromatogram after 200 injections of a typical polyamide sample. The chromatogram did not differ significantly from the first injections.

5. Optimization of the oligomer separation

To optimize the separation of the first six linear and six cyclic oligomers, a framework has to be defined, which fulfills three separation requirements.

First, the polar 6-aminocaproic acid is difficult to separate from the excess formic acid used to dissolve and to inject the polyamide properly on an octadecyl modified silica-based column. To retain and separate this linear monomer very low organic modifier concentrations should be used.

Second, for a fully selective determination of all oligomers the first six cyclic oligomers should be separated from all linear oligomers within approximately 45 min. The first six linear oligomers do not need to be separated from all cyclic oligomers (i.e.

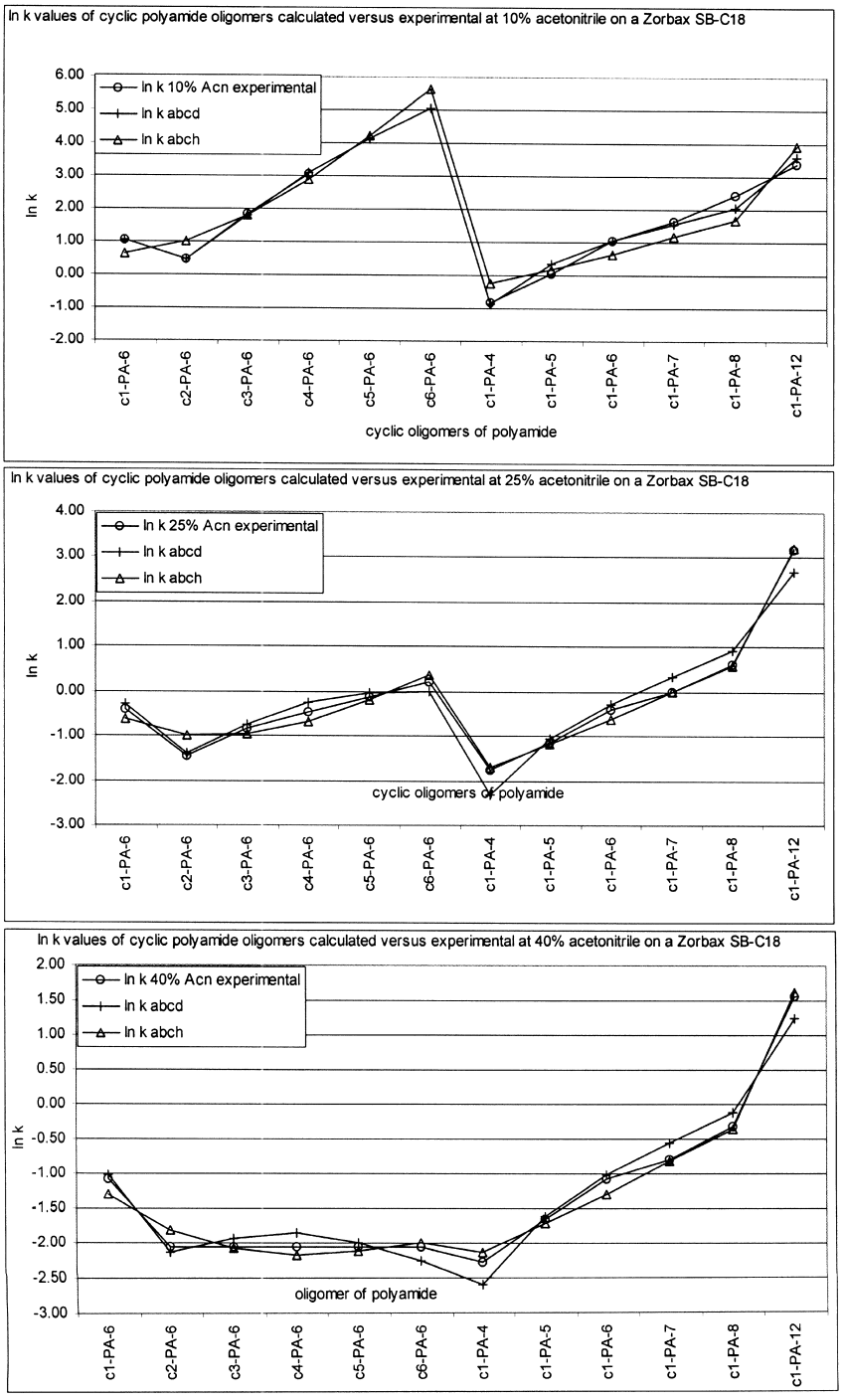

Fig. 7. Retention model $\ln k = aV^{2/3} + b\Delta G + c + hH$ and $\ln k = aV^{2/3} + b\Delta G + c + dD$ versus the experimental values of the cyclic oligomers of polyamide-6 and the cyclic monomers of PA-4, PA-5, PA-6, PA-7, PA-8 and PA-12 at 10, 25 and 40% acetonitrile. The abch and abcd parameters were calculated using multiple regression of the retention factors of the cyclic monomers and oligomers.

Table 5
Elution time of different often used dead volume markers

φ Acetonitrile in aqueous 10 m*M* H_3PO_4	t_{uracil} (min)	$t_{thiourea}$ (min)	$t_{formamide}$ (min)	$t_{nitrate}$ (min)
1%	4.045	2.460	2.309	2.091
5%	2.811	2.338	2.200	2.048
10%	2.382	2.252	2.137	2.003
25%	2.049	2.092	2.017	1.865
40%	1.906	1.968	1.913	1.716
50%	1.858	1.930	1.889	1.635

Measurements were performed on a 250×4 mm Nucleosil 120-5C_{18} column at room temperature with a flow-rate of 1.0 ml/min.

higher cyclic oligomers $n>6$), because the linear oligomers are detected selectively with post-column reaction detection [2]. When the linear oligomers could be retained selectively and elute after elution of the first six cyclic oligomers, the first six linear and cyclic oligomers can selectively be determined. If no selective retention of the linear oligomers is used, the first six cyclic oligomers need to be separated from approximately eight linear oligomers.

Third, the separation of the cyclic monomer and cyclic dimer is most important. Even when a large amount of cyclic monomer is present in, e.g. unwashed polyamide-6 samples, a baseline separation with the cyclic dimer is necessary.

5.1. Linear solvent strength model

To optimize a separation, varying the gradient steepness is probably the first choice. Commercial software is available to perform this optimization (e.g. DryLab, Chromsword). A linear correlation between the logarithm of the retention factor and the modifier concentration, the so-called Soczewinski–Wachtmeister relation [37], which is also known as the linear solvent strength (LSS) model is used for this optimization purpose. However, as can be seen in Fig. 3a this correlation is in this case not linear at all. Commercially available software also presumes a fixed dead volume of the column and an instantaneous equilibration of the chromatographic system during gradient elution. However, in reversed-phase systems with octadecyl modified silica this measured dead volume changes with the amount of modifier.

In Table 5, the elution times of some often used dead volume markers are compared. From these results it is clear that different t_0 markers could yield different t_0-values. Thiourea was used as a t_0 marker in all experiments as its UV spectrum deviates clearly from the polyamide oligomers and its elution time at higher percentage modifier equals the elution time of the higher cyclic oligomers of polyamide-6 ($n=2$–6). Observing the retention time of this marker under different experimental conditions, again no fixed dead volume is obtained using an octadecyl modified stationary phase (Table 6). However, on butyl modified silica, the dead volume is much more constant for the different percentages of modifier. The average dead time of this column was 2.41±0.01 min ($n=24$) with a standard deviation of 0.03 min.

The dwell volume of a chromatographic system is defined as the volume needed before the gradient

Table 6
Elution time of t_0 marker thiourea under different experimental conditions

Modifier (%)	t_0 (min)							
	250×4 mm Nucleosil 120-5C_{18}				250×4 mm Nucleosil 120-5C_4			
	Acetonitrile		Methanol		Acetonitrile		Methanol	
	RT	40°C	RT	40°C	RT	40°C	RT	40°C
1	2.46	2.34	2.48	2.35	2.41	2.38	2.41	2.35
5	2.34	2.25	2.39	2.29	2.41	2.39	2.40	2.39
10	2.25	2.17	2.32	2.24	2.41	2.38	2.41	2.39
25	2.09	2.04	2.22	2.16	2.41	2.41	2.41	2.41
40	1.99	1.94	2.17	2.12	2.40	2.37	2.45	2.42
50	1.93	1.91	2.15	2.10	2.40	2.46	2.46	2.43

RT, Room temperature.

Table 7
The conditions by which the gradient conditions were calculated

Experiment	Modifier	Column	Column temperature
1	Acetonitrile	250×4 mm Nucleosil 120-5C_{18}	RT
2	Acetonitrile	250×4 mm Nucleosil 120-5C_{18}	40°C
3	Methanol	250×4 mm Nucleosil 120-5C_{18}	RT
4	Methanol	250×4 mm Nucleosil 120-5C_{18}	40°C
5	Acetonitrile	250×4 mm Nucleosil 120-5C_4	RT
6	Acetonitrile	250×4 mm Nucleosil 120-5C_4	40°C
7	Methanol	250×4 mm Nucleosil 120-5C_4	RT
8	Methanol	250×4 mm Nucleosil 120-5C_4	40°C

Aqueous part of the mobile phase is 10 m*M* phosphoric acid. Flow-rate 1.0 ml/min; RT, room temperature.

change reaches the top of the column. This volume can easily be determined by tracking the mobile phase changes. However, when this tracking of the mobile phase is performed at the column outlet, one could expect a larger difference than just the dead volume, as a part of the organic modifier will be adsorbed to the stationary phase. By measuring the conductivity of the eluent during the gradient at the end of the column, this solvent uptake was estimated for a gradient of 1–75% modifier with a gradient time of 10 min. No significant differences of the programmed and observed gradient end time were observed when the gradient time was changed to 60 min. The results of different experimental set-ups (Table 7) are compared in Table 8, which is graphically depicted in Fig. 8 for a Nucleosil 120-5C_{18} column with an acetonitrile gradient at ambient temperature. As can be seen, the measured dwell volume of 0.58 ml increases in all experiments due to the preferential solvent uptake. However, the difference of the post-column observed end time and the programmed end time is in all cases smaller compared to the difference observed between the post-column observed start time and the programmed start time. This suggests a larger dwell volume than measured and a steeper gradient than programmed. To calculate the gradient retention times from isocratic data Eq. (5) has to be solved [20]:

$$\int_0^{t'_r} \frac{dt}{t_0 k} = 1 - x \tag{5}$$

Table 8
Observed gradient time is calculated as the observed end time minus the t_0 value at 75% subtracted from the observed start time minus the t_0 value at 1% modifier = (12.40 − 1.93) − (3.80 − 2.46) = 9.13

	250×4 mm Nucleosil 120-5C_{18}				250×4 mm Nucleosil 120-5C_4			
	Acetonitrile		Methanol		Acetonitrile		Methanol	
	RT	40°C	RT	40°C	RT	40°C	RT	40°C
Observed start time (post column) (min)	3.80	3.83	3.35	3.25	3.40	3.30	3.25	3.15
Observed end time (post column) (min)	12.40	12.40	12.85	12.80	13.10	13.00	13.20	13.20
t_0 (1% modifier) (min) = start gradient	2.46	2.34	2.48	2.35	2.41	2.38	2.41	2.35
t_0 (75% modifier) (min) = end gradient	1.93	1.91	2.15	2.10	2.40	2.36	2.46	2.43
Observed/corrected gradient time (min)	9.13	9.00	9.83	9.80	9.71	9.72	9.90	9.97
Observed/corrected dwell time (min)	1.34	1.49	0.87	0.90	0.99	0.92	0.84	0.80

Observed dwell time = 3.80 − 2.46 = 1.34.

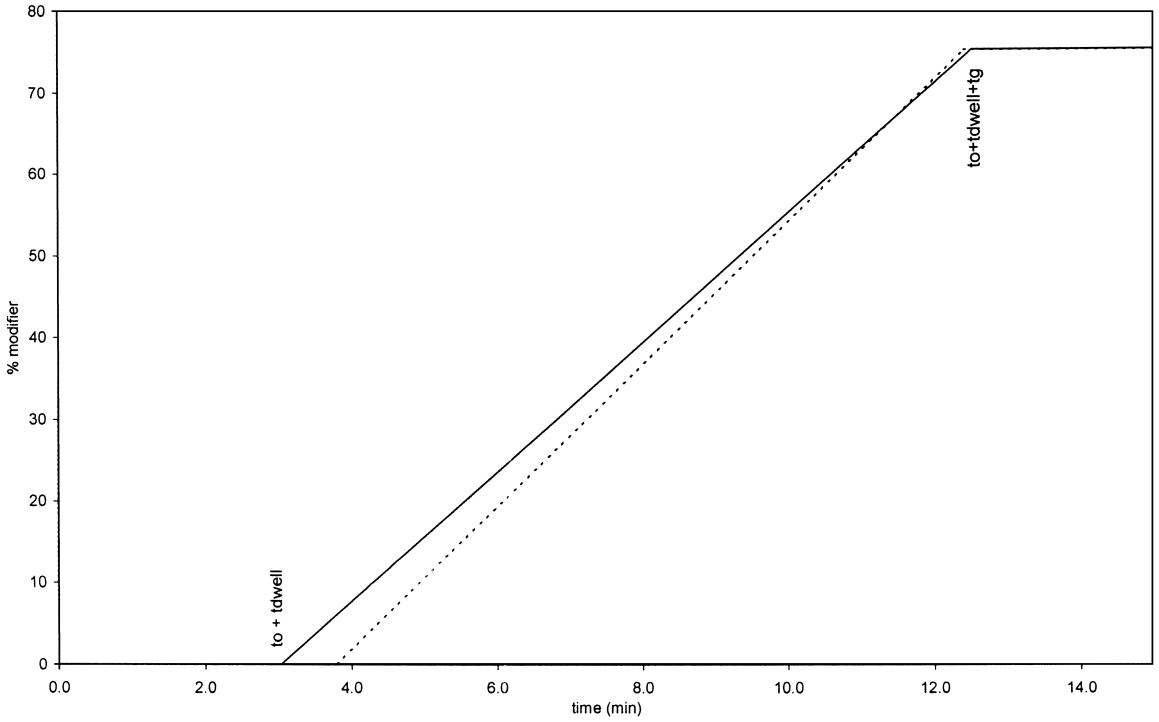

Fig. 8. Computerized model of the modifier concentration in 10 m*M* phosphoric acid as the aqueous part, measured using a conductivity detector at the end of the column (Nucleosil 120-5C_{18}). Straight line, programmed gradient profile; dashed line, observed linearized gradient profile (measured at 0 and 100% modifier).

where t_0 is the column dead time, t'_r is the net retention time (retention time minus the column dead time), k is the retention factor and x is the fraction of the column, that has been past by the component before the gradient actually reaches the column. x is defined as [20]:

$$x = \frac{t_D}{t_0 k_0} \tag{6}$$

where t_D is the dwell time, which is the time necessary for the gradient to reach the top of the column and k_0 which is the retention factor of the component at the starting conditions of the gradient with the starting modifier fraction φ_0.

The LSS model uses a linear relation between log k and the modifier concentration ($\log k = \log k_w - S\varphi$) and the retention time t_r can be calculated using Eq. (7) [20]:

$$t_r = t_D + \frac{t_0}{b} \cdot \log[2.3\, k_0 b(1-x) + 1] + (1-x)t_0 \tag{7}$$

where $b = (t_0 \Delta\varphi\ S/t_g)$ and $\log k_0 = \log k_w - S\varphi_0$ where k_w is the retention factor at 100% water, $\Delta\varphi$ is the difference of the starting and end concentration of the modifier fraction during the linear gradient and t_g is the gradient time.

When a second-order polynomial relation is used ($\log k = A0 - A1\varphi + A2\varphi^2$), the integral is still solvable, but the second-order polynomial constants cannot be calculated from gradient data and iterative methods must be used [38,39]. However, the polynomial constants can be calculated from isocratic data (1, 5, 10, 25, 40 and 50% modifier) and with easy iterative procedures retention times of gradient elutions can be calculated. By using iterative procedures, it is also possible to use higher polynomial models and to use drifting t_0-values. In Table 9, the calculated data are given for the cyclic monomer on a Nucleosil 120-5C_{18} column at room temperature with acetonitrile as modifier. In addition to the programmed gradient time and standard dwell volume, the post-column observed gradient time and

Table 9
Calculated versus measured retention times of the cyclic monomer at different gradient times (t_g in min) with a gradient from 1 to 75% acetonitrile

Model	Order of polynomial	t_0	Programmed conditions, $t_{dwell}=0.58$ min, $t_{g\ programmed}$				Observed conditions corrected for acetonitrile uptake, $t_{dwell\ observed}=1.34$ min, $t_{g\ observed}$			
			$t_g=10$	$t_g=20$	$t_g=40$	$t_g=60$	$t_g=9.13$	$t_g=19.13$	$t_g=39.13$	$t_g=59.13$
1	1	Fixed	7.00	9.00	11.40	12.87	7.37	9.38	11.75	13.18
2	1	Variable	6.46	8.42	10.80	12.28	6.85	8.83	11.18	12.62
3	2	Fixed	6.30	8.08	10.60	12.44	6.77	8.58	11.11	12.93
4	2	Variable	5.83	7.60	10.11	11.94	6.32	8.12	10.63	12.45
5	4	Fixed	6.24	7.80	10.05	11.75	6.75	8.34	10.59	12.29
6	4	Variable	5.75	7.32	9.57	11.28	6.26	7.86	10.12	11.82
Measured retention time (min)			6.17	7.85	10.13	11.81	6.17	7.85	10.13	11.81

The calculated retention times were obtained from the isocratic data (1, 5, 10, 25, 40 and 50% acetonitrile).

dwell volume have also been used to calculate the retention time. Six different models were used. Three different polynomials to describe the relation between the log k and organic modifier concentration were used, each with fixed and variable t_0 values. It can be seen that the calculated retention times with the fourth-order polynomial with changing t_0 values but without the dwell-time and gradient corrections does not give the best fit with the experimentally observed retention times (Table 9). However, when a correction for the acetonitrile uptake in the stationary phase is made, this model does give the best results.

These calculations where also performed for the cyclic monomer and cyclic dimer under the different experimental conditions of Table 7. For every model given in Table 9 four different gradient retention times ($t_g=10$, 20, 40 and 60 min) for the two components (cyclic monomer and cyclic dimer of polyamide-6) were calculated using the eight experimental conditions of Table 7 given 64 results. The percentile deviations from the measured retention times are given in Fig. 9a for uncorrected gradient times and dwell volumes. Fig. 9b depicts the use of corrected gradient times and dwell volumes. For the lower order models a bimodal distribution can be observed. All results obtained on the Nucleosil 120-5C_4 column show much better fits for all models compared to the Nucleosil 120-5C_{18} column. This is easily explained as the t_0-values on the Nucleosil 120-5C_4 column are not so much influenced by the modifier concentration (the largest difference of two measured t_0-values in an experiment is always smaller as 0.08 min) and the $\ln k - \varphi$ relation approaches a linear behavior, resulting in much better fits for all models. By correcting the data for the modifier uptake on the stationary phase, the calculated retention times increased approximately 0.5–2% for experiment 3–8 of Table 8. However for experiments 1–2 of Table 8 where acetonitrile was used on a Nucleosil 120-5C_{18} phase the calculated retention times increased 6–8%. From Fig. 9a,b, it can be concluded that higher polynomials improve accuracy and also improve precision if gradient retention time data are calculated from isocratic measurement. As the distribution of the fourth-order polynomial is smaller if variable t_0-values are used, this model seems to give the best precision. However, a substantial number of calculated retention times with the fourth-order polynomial (variable t_0 and corrected gradient and dwell times) deviated more than 2% of the measured gradient retention time (see + in Fig. 9b).

Gradient retention times (with $t_g=20$ and 40 min) were also calculated with the LSS model from two initial gradient runs ($t_g=10$ and 60 min) using commercially available software. These results are given in Table 10. Although Chromsword and DryLab calculate exactly the same retention time, they calculate different peak widths, resulting in different proposed resolutions. However, for both programs an average deviation in the calculated resolution of 0.4 unit was obtained. Although a linear behavior of the $\ln k - \varphi$ relation and a fixed dead volume is assumed (both assumptions are not ful-

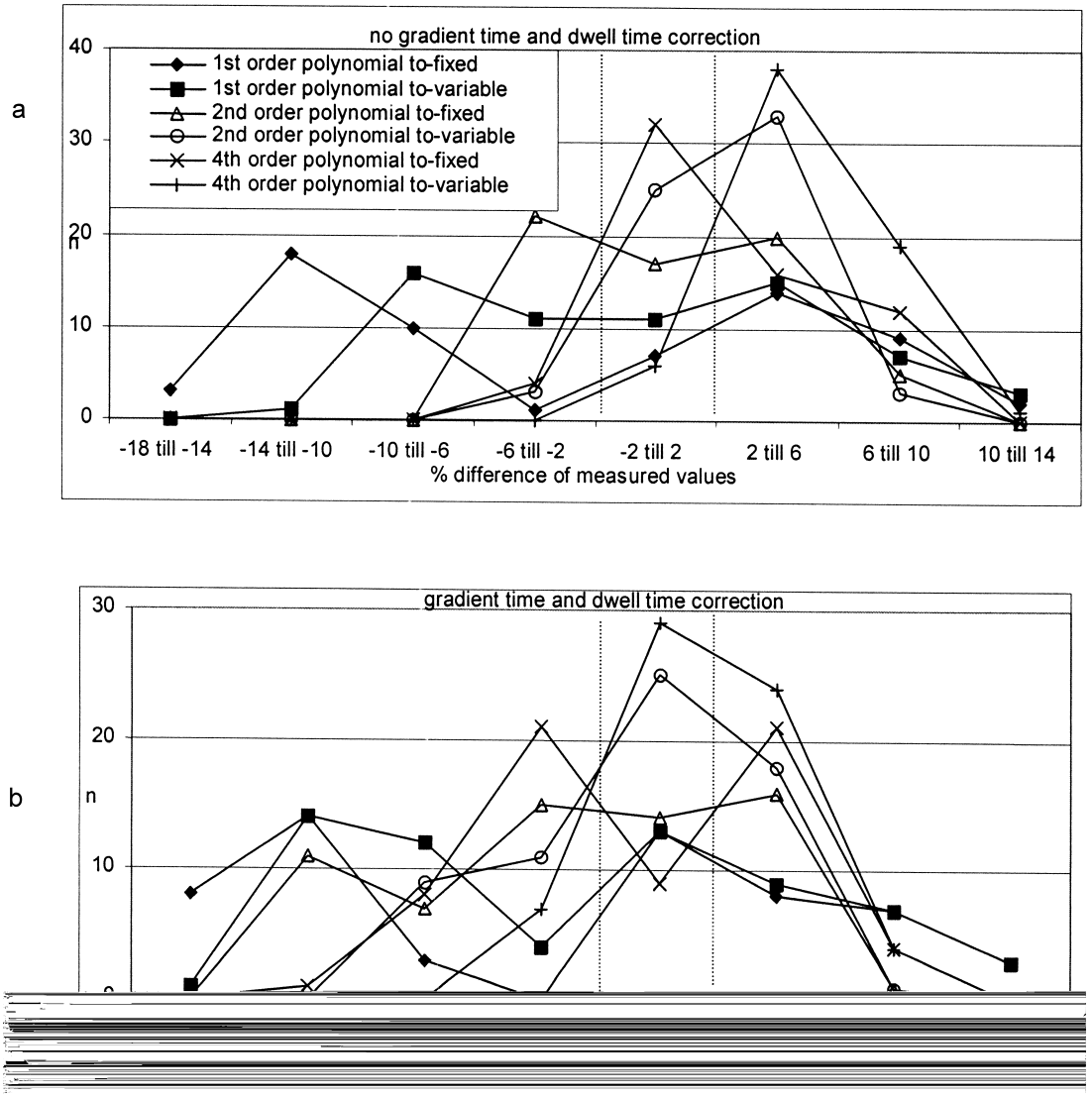

Fig. 9. Distribution of the observed errors between calculated and observed retention times of the cyclic monomer and cyclic dimer of polyamide-6 using uncorrected dwell time (0.58 min) and gradient times ((a) $t_g = 10$, 20, 40 and 60 min) at the experimental conditions given in Table 7. (b) uses the corrected gradient times and corrected dwell volumes of Table 8. The ln $k - \varphi$ relations in (a) and (b) were obtained from isocratic data at 1, 5, 10, 25, 40 and 50% modifier. ♦1st order polynomial and fixed t_0 value; ■ 1st order polynomial and variable t_0 value; ▽ 2nd order polynomial and fixed t_0 value; ○ 2nd order polynomial and variable t_0 value; × 4th order polynomial and fixed t_0 value; + 4th order polynomial and fixed t_0 value.

filled in exp. 1–4) and no corrections were made for excess solvent uptake by the stationary phase, it can also be concluded that the deviation of the predicted resolution is almost always less than 0.8.

5.2. Gradient optimization

To perform a good optimization of the first six linear and cyclic oligomers, stable conditions with

used to effectively remove all polyamide from the stationary phase, resulting in stable retention times during a sequence of gradient runs.

It was demonstrated that gradient retention times could not be calculated accurately using the LSS model and isocratic input data. Although higher polynomials gave better fits, a direct translation of the isocratic data to gradient retention times did not yield accurate retention times. However, the LSS model could be used for the optimization of the separation of the first six linear and cyclic oligomers of polyamide-6, although a significant non-linearity of the elution of the cyclic monomer and dimer was observed. The prediction of the LSS model, using interpolation of the gradient data, resulted in an average error of 0.4 resolution units.

Acknowledgements

We would like to thank Dr S. Galushko for helpful discussions.

References

[1] Y. Mengerink, R. Peters, M. Kerkhoff, J. Hellenbrand, H. Omloo, J. Andrien, M. Vestjens, Sj. van der Wal, J. Chromatogr. A 876 (2000) 37.
[2] Y. Mengerink, R. Peters, M. Kerkhoff, J. Hellenbrand, H. Omloo, J. Andrien, M. Vestjens, Sj. van der Wal, J. Chromatgr. A 878 (2000) 45.
[3] L.R. Snyder, in: E. Heftmann (Ed.), Chromatography 5th ed. Fundamentals and applications of Chromatography and Related Differential Migration Methods, Part A: Fundamentals and Techniques (Journal of Chromatography Library, Vol. 51A), Elsevier, Amsterdam, 1992, p. A1.
[4] Sj. van der Wal, LC–GC 5 (1992) 36.
[5] Y. Mengerink, H.C.J. de Man, Sj. van der Wal, J. Chromatogr. 552 (1991) 593.
[6] R. Kulkarni, P. Kanekar, Process Control Qual. 9 (1997) 31.
[7] R.N. Nikolov, N.I. Angelova, D.I. Pishev, Khim. Volokna 5 (1992) 57.
[8] C. Guaita, Makromol. Chem. 185 (1984) 459.
[9] C.T. Barkby, G. Lawson, Food Addit. Contam. 10 (1993) 541.
[10] S.V. Galuskho, J. Chromatogr. 552 (1991) 19.
[11] S.V. Galushko, I. Shishkina, Chromatographia 36 (1993) 39.
[12] S.V. Galushko, A.A. Kamenchuk, G.L. Pit, J. Chromatogr. A 660 (1994) 47.
[13] Cs. Horváth, W. Melander, I. Molnar, J. Chromatogr. 125 (1976) 129.
[14] Cs. Horváth, W. Melander, J. Chromatogr. Sci. 15 (1977) 393.
[15] R. Kaliszan, Structure and Retention in Chromatography, A Chemometric Approach, Harwood, Australia, 1997.
[16] P. Schoenmakers, in: E. Katz, R. Eksteen, P. Schoenmakers (Eds.), Handbook of HPLC (Chromatographic Science Series, Vol. 78), Marcel Dekker, New York, 1998, p. 93.
[17] L.R. Snyder, J. Chromatogr. 13 (1964) 415.
[18] L.R. Snyder, J.W. Dolan, J.R. Gant, J. Chromatogr. 165 (1979) 3.
[19] L.R. Snyder, J.W. Dolan, J.R. Gant, J. Chromatogr. 165 (1979) 31.
[20] L.R. Snyder, J.W. Dolan, Adv. Chromatogr. 38 (1998) 115.
[21] J.W. Dolan, L.R. Snyder, N.M. Djordjevic, D.W. Hill, T.J. Waeghe, J. Chromatogr. A 857 (1999) 1.
[22] J.W. Dolan, L.R. Snyder, N.M. Djordjevic, D.W. Hill, T.J. Waeghe, J. Chromatogr. A 857 (1999) 21.
[23] J.W. Dolan, L.R. Snyder, R.G. Wolcott, P. Haber, T. Baczek, R. Kaliszan, L.C. Sander, J. Chromatogr. A 857 (1999) 21.
[24] P.L. Zhu, J.W. Dolan, L.R. Snyder, N.M. Djordjevic, D.W. Hill, L.C. Sander, T.J. Waeghe, J. Chromatogr. A 756 (1996) 21.
[25] P.L. Zhu, J.W. Dolan, L.R. Snyder, J. Chromatogr. A 756 (1996) 41.
[26] P.L. Zhu, L.R. Snyder, J.W. Dolan, D.W. Hill, L. van Huekelem, T.J. Waeghe, J. Chromatogr. A 756 (1996) 51.
[27] P.L. Zhu, L.R. Snyder, J.W. Dolan, N.M. Djordjevic, D.W. Hill, J.T. Lin, L.C. Sander, T.J. Waeghe, J. Chromatogr. A 756 (1996) 63.
[28] R.G. Wolcott, J.W. Dolan, LC–GC Int. (2000) 14.
[29] P.J. Schoenmakers, H.A.H. Billiet, L. de Galan, J. Chromatogr. 205 (1981) 13.
[30] M.A. Quarry, R.L. Grob, L.R. Snyder, J. Chromatogr. 285 (1984) 19.
[31] P.J. Schoenmakers, H.A.H. Billiet, L. de Galan, J. Chromatogr. 185 (1979) 179.
[32] Y.V. Kazakevich, H.M. McNair, J. Chromatogr. Sci. 31 (1993) 317.
[33] Y.V. Kazakevich, H.M. McNair, J. Chromatogr. Sci. 33 (1995) 321.
[34] H. Engelhardt, M. Arangio, T. Lobert, LC–GC Int. 10 (1997) 803.
[35] R. Puffr, V. Kubanek, in: Lactam-Based Polyamides, Vol. I, CRC Press, Boston, 1990.
[36] Y. Mengerink, Sj. van der Wal, H.A. Claessens, C.A. Cramers, J. Chromatogr. A 871 (2000) 259.
[37] E. Soczewinski, C.A. Wachtmeister, J. Chromatogr. 7 (1962) 311.
[38] P.J. Schoenmakers, H.A.H. Billiet, R. Tijssen, L. de Galan, J. Chromatogr. 149 (1978) 519.
[39] M. Abramowitz, I. Stegum, Handbook of Mathematical Functions, Dover, New York, 1970, p. 303.
[40] R. LoBrutto, A. Jones, Y.V. Kazakevich, H.M. McNair, J. Chromatogr. A 913 (2001) 173.